Contents list available at **IJND**

International Journal of Nano Dimension

Journal homepage: *www.IJND.ir*

Investigation of flow and heat transfer of nanofluid in a diverging sinusoidal channel

M. Falahaty Naghibi[1]
M. Rahimi-Esbo[2, *]
R. Mohammadyari[2]
K. Mobini[1]

[1]*School of Mechanical Enginnering, Shahid Rajaee Teacher Training University, Tehran, Iran.*

[2]*Young Researchers and Elite Club, Buin Zahra Branch, Islamic Azad University, Buin Zahra,*

* Corresponding author:
Mazaher Rahimi-Esbo
Young Researchers and Elite Club, Buin Zahra Branch, Islamic Azad University, Buin Zahra, Iran.
Tel +98 2834226114
Fax +98 2834225316
Email rahimi.mazaher@gmail.com

ABSTRACT

Using of nanofluids and ducts with corrugated walls are both supposed to enhance heat transfer, by increasing the heat transfer fluid conductivity and the heat transfer area respectively. Use of a diverging duct with a jet at inlet section may further increase heat transfer by creating recirculation zones inside the duct. In this work two-dimensional incompressible laminar flow of a nanofluid entering a diverging channel with sinusoidal walls through a jet at inlet section, is numerically investigated. Effects of aspect ratio (duct-to-jet height ratio), wall-wave amplitude, wall wavelength, Reynolds number, nanoparticle volume fraction and the size of nanoparticles on the flow structure and heat transfer are investigated. The results show that by increasing the Reynolds number, wall wave amplitude and nanoparticle volume fraction, the duct averaged Nusselt number will increase, while the wall wavelength and the particle size have an adverse effect. The inlet jet has the strongest effect on heat transfer at the aspect ratio of 4.

Keywords: *Heat transfer enhancement; Laminar flow; Nanofluid; Diverging channel; Sinusoidal channel.*

INTRODUCTION

Changing the fluid properties and the flow geometry are two common ways of making an improvement in heat transfer rate. Using porous media and micro scale channels, increasing the surface area and placing a shackle in the way of fluid are different ways of increasing heat transfer by changing the geometry. Heat transfer fluid plays a very important role in many industries including power stations, production processes, transportation and electronics. The conventional methods of heat transfer enhancement are based on the structure variation such as increase of heat transfer area, vibration of heat transfer surface, injection or suction of fluid and application of electrical or magnetic fields. These enhancement techniques can hardly meet the astronomical increase in demand for heat transfer enhancement.

Therefore, in the last decade many researchers worked on the new heat transfer fluids, including nanofluids. Nanofluids are made by adding a small amount of tiny particles (in nanometer scale, normally up to 100nm) to a liquid. This may increase thermal conductivity and other heat transfer properties of the liquid. This could lead to a revolution in heat transfer applications in near future. Fluids with suspended nanoparticles are called nanofluid; a term proposed by Choi [1] of the Argonne National Laboratory, USA. Nanofluids can be considered as the next generation heat transfer fluids, because they offer exciting new possibilities to enhance heat transfer performance compared to pure liquids. They are expected to have superior properties compared to conventional heat transfer fluids, as well as fluids containing micro-sized metallic particles. The much larger relative surface area of nanoparticles, compared to those of conventional particles, not only significantly improves heat transfer capabilities, but also increases stability of the suspension. Nanofluids can improve abrasion-related properties compared to the conventional solid-fluid mixtures. To explain the reasons for the anomalous increase of thermal conductivity in nanofluid, Keblinski *et al.* [2] proposed four possible mechanisms: Brownian motion of the nanoparticles, molecular-level layering of the liquid at the liquid-particle interface, the nature of heat transport in the nanoparticles and the effects of nanoparticles clustering.

Some researchers applied homogenous nanofluid flow in different applications. Rahimi-Esbo *et al.* [3] numerically studied, forced convection of turbulent nanofluid flow in a head box. Their results showed that by increasing the Reynolds number, aspect ratio and the particle volume fraction, the average Nusselt number is increased. They assumed the nanoparticles and the base fluid (i.e. water) to be in thermal equilibrium and noslip occurs between them. Also Rahimi-Esbo *et al.* [4] studied forced convection of turbulent jet flow in a converging sinusoidal channel and reported the same results. Wang and Chen [5] analyzed the rate of heat transfer for flow through a sinusoidal converging-diverging channel using a simple coordinate transformation method and the spline alternating-direction implicit method. They studied the effects of wave geometry, Reynolds number and Prandtl number on skin friction and

Nusselt number. They observed that as the wave amplitude and the wavelength and the Reynolds number increase, the total heat transfer and the local Nusselt number increase in the converging-diverging part of the channel. They concluded that a corrugated channel is an effective heat transfer enhancement device. Koand Cheng [6] numerically investigated the developing laminar forced convection and entropy generation in a wavy channel. The effects of aspect ratio and the Reynolds number on entropy generation were their major concerns. Their result demonstrated the enhancement in heat transfer by increasing aspect ratio and Reynolds number. Flow through a channel with sinusoidal plates was experimentally investigated by Oviedo-Tolentino *et al.* [7]. The experiments were operated in a water tunnel .Laser illuminated particle tracking was used as the technique of flow visualization. They reported that, for a set of flow and geometric parameters, eight waves were enough to develop the flow in the channel used for their study. Chang *et al.* [8] experimentally studied enhancement of heat transfer in a radially rotating furrowed channel with two opposite walls. Their results include Nusselt number scans which were generated by means of infra-red thermographs over two opposite leading and trailing wavy walls of a radially rotating furrowed channel. For the transverse and skewed wavy channels at $1000 < Re < 2000$, the Nusselt number ratios were between 5 and 8.8 and between 5.4 and 11.3, respectively.

Choi and Suzuki [9] applied large eddy simulation (LES) to study the thermal field of a turbulent flow in a channel having one wavy wall with various wall wave amplitudes. They showed that both the friction coefficient and the Nusselt number have maximum values in the upper part of the wavy wall. Wall bending was found to effectively enhance the wall heat transfer. Heris *et al.* [10] experimentally investigated laminar flow forced convection heat transfer of Al_2O_3-water in a circular tube with constant wall temperature. The Nusselt numbers were obtained for different nanoparticle concentrations as well as various Peclet and Reynolds numbers. Experimental results emphasize the enhancement of heat transfer due to the presence of nanoparticles in the fluid. Heat transfer coefficient was increased by increasing the concentration of nanoparticles in nanofluid. The increase in heat transfer coefficient due to the

presence of nanoparticles is much higher than the prediction of single phase heat transfer correlation used with nanofluid properties. Hwang *et al.* [11] measured the pressure drop and convective heat transfer coefficient of a water-Al_2O_3nanofluidflowing through a uniformly heated circular tube in fully developed laminar flow regime. Experimental results show that the convective heat transfer coefficient enhancement exceeds, by a large margin, the thermal conductivity enhancement. They proposed that flattening of the velocity profile is a possible mechanism for the convective heat transfer coefficient. Al-Aswadi *et al.* [12] investigated laminar forced convection flow of different nanofluids over a 2D horizontal backward facing step placed in a duct. They reported that the reattachment point moves downstream far from the step as the Reynolds number increases. They also found that the nanofluid containing SiO_2 nanoparticles has the highest velocity among the other nanofluid types, while nanofluid of Au nanoparticles has the lowest velocity.

Santra *et al.* [13] simulated copper-water nanofluid flow in an isothermally two-dimensional rectangular duct. They investigated the effect of Newtonian as well as non-Newtonian fluid for a wide range of Reynolds number and nanoparticles volume fraction. They reported that heat transfer increases by increasing of the solid volume fraction for any Reynolds number. This increment was more or less the same for both Newtonian and non-Newtonian nanofluid, particularly for lower Reynolds number. A numerical investigation of heat transfer and flow field in a wavy channel with a nanofluid was performed by Heidary and Kermani [14]. They reported that adding nanoparticles to the base fluid and application of wavy walls can significantly enhance heat transfer. They also observed that the skin friction coefficient is almost insensitive to the volume fraction of nanoparticles. However, they only studied the effect of amplitude on heat transfer. It seems that studying the effects of amplitude alone is not enough to fully understand this problem, and more comprehensive investigations are still required.

Khoshvaght *et al.* analyzed heat transfer and flow characteristics of the sinusoidal-corrugated channel with Al_2O_3-water nanofluid by a 2-D numerical simulation. They used a parametric study method to analyze the performance of

sinusoidal-corrugated channel in practical applications like plate-fin compact heat exchangers [15-19]. They evaluated the effects of channel height, channel length, wave length, wave amplitude, and phase shift at different Reynolds numbers (6000–22,000) and nanoparticle volume fractions (0–4%). Nusselt number and Darcy friction factor are considered as performance parameters. They reported that the channel height and wave amplitude have the highest influences on Nusselt number and friction factor values, respectively. Also, their results show that the nanofluid flow inside the sinusoidal-corrugated channels offers higher values of Nusselt number compared to the base fluid, while the friction factor of both the nanofluid and the base fluid gets almost the same values. Also they proposed correlations to predict Nusselt number and friction factor of the water and Al2O3-water nanofluid flows in the sinusoidal-corrugated channels.

Ahmed *et al.* [20] numerically studied the flow and heat transfer characteristics of CuO–water nanofluid for straight and corrugated channels with sinusoidal, triangular and trapezoidal corrugations. They solved numerically the governing continuity, momentum and energy equations in terms of body-fitted coordinates are using finite volume approach. They investigated the effect of nanoparticles volume fraction and Reynolds number on the stream wise velocity contours, temperature contours, average Nusselt number, non-dimensional pressure drop, and thermal–hydraulic performance factor. Their result show that the average Nusselt number and thermal–hydraulic performance factor increases with increasing nanoparticles volume fraction and Reynolds number for all channel shapes. Also the non-dimensional pressure drop increases with increasing nanoparticles volume fraction, while it decreases as Reynolds number increases for all channel shapes. Furthermore, they reported the trapezoidal channel has the highest Nusselt number and followed by the sinusoidal, triangular and straight channel.

Ahmed *et al.* [21] numerically investigated laminar copper–water nanofluid flow and heat transfer in a two-dimensional wavy channel. The Reynolds number and nanoparticle volume fraction considered were in the ranges of 100–800 and 0–5% respectively. They analyzed the effects of nanoparticle volume fraction, the wavy channel amplitude and wavelength and the Reynolds

number on the local skin-friction coefficient, local and average Nusselt number and the heat transfer enhancement. Their Results showed that the friction coefficient and Nusselt number increase as the amplitude of wavy channel increases. As the nanoparticle volume fraction increases, the Nusselt number was found to be significantly increased, accompanied by only a slight increase in the friction coefficient. Also they founded that the enhancement in heat transfer mainly depends on the nanoparticle volume fraction, amplitude of the wavy wall and Reynolds number rather than the wavelength.

In this work laminar flow of water-Al$_2$O$_3$ nanofluid is numerically simulated in a diverging rectangular channel with two sinusoidal walls. For this purpose the governing equations were discretized and solved using finite volume and a SIMPLE based method. Effects of aspect ratio, amplitude of sinusoidal walls, the wavelength of sinusoidal walls, Reynolds number, nanoparticle volume fraction and diameter of nanoparticles on the Nusselt number have been studied.

EXPERIMENTAL

Physics of the problem and governing equations

The geometry of the problem as shown in Figure 1 is a rectangular channel with two flat parallel walls at the sides and two wavy diverging walls at the top and the bottom. The fluid enters the channel through a rectangular jet located at the channel inlet on the left. The jet width is equal to the channel width and its height could be equal or less than the channel inlet height. The channel width is constant throughout the channel length. The wavy walls are isothermal and the side walls are adiabatic. The equation describing the wavy walls (shown in Figure 1) is a function of amplitude and wavelength.

The continuity, momentum and energy equations for the present 2D incompressible flow can be expressed as:

$$\frac{\partial u}{\partial x} + \frac{\partial v}{\partial y} = 0 \tag{1}$$

$$u\frac{\partial u}{\partial x} + v\frac{\partial u}{\partial y} = -\frac{1}{\rho_{nf}}\frac{\partial p}{\partial x} + \upsilon_{nf}(\frac{\partial^2 u}{\partial x^2} + \frac{\partial^2 u}{\partial y^2}) \tag{2}$$

$$u\frac{\partial v}{\partial x} + v\frac{\partial v}{\partial y} = -\frac{1}{\rho_{nf}}\frac{\partial p}{\partial y} + \upsilon_{nf}\left(\frac{\partial^2 v}{\partial x^2} + \frac{\partial^2 v}{\partial y^2}\right) \tag{3}$$

$$u\frac{\partial T}{\partial x} + v\frac{\partial T}{\partial y} = \alpha_{nf}\left(\frac{\partial^2 T}{\partial x^2} + \frac{\partial^2 T}{\partial y^2}\right) \tag{4}$$

The boundary conditions for this kind of flow are:

$$\frac{\partial T}{\partial x} = 0, \ \frac{\partial u}{\partial x} = 0 \text{ for the outlet surface} \tag{5}$$

$$T = T_w, \ u = v = 0 \text{ for the isothermal walls} \tag{6}$$

$$\frac{\partial T}{\partial \hat{n}} = 0, \ u = v = 0 \text{ for the adiabatic walls} \tag{7}$$

The Reynolds number is defined by:

$$\text{Re} = \frac{\rho_f U_{in} h}{\mu_f}. \tag{8}$$

The characteristics length h is the average height of the channel.
The local Nusselt number is defined by:

$$Nu_x \quad -\frac{k_{nf}}{k_f}\frac{h(\partial T/\partial \hat{n})}{T_{bulk} - T_w} \tag{9}$$

$\frac{\partial T}{\partial \hat{n}}$ is the temperature gradient normal to the walls

$$\frac{\partial T}{\partial \hat{n}} = \vec{\nabla}T.\hat{n} \tag{10}$$

T_{bulk} is the mean temperature and can be calculated as defined below:

$$T_{bulk} = \frac{\int_{A_c} \rho u c_f T dA_c}{\dot{m}c_f} \tag{11}$$

The thermal conductivity of the nanofluid is calculated from Chon et al. (2005), which is expressed in the following form:

$$\frac{k_{nf}}{k_f} = 1 + 64.7\phi^{0.746}(d_f/d_p)^{0.369} \times (k_p/k_f)^{0.7476} \Pr_f^{0.9955} \mathrm{Re}_p^{1.2321}$$

(12)

Prandtl number of the base fluid and the particles Reynolds number are defined by:

$$\Pr_f = \mu_f / \rho_f \alpha_f \quad (13)$$

$$\mathrm{Re}_p = \rho_f k_b T / 3\pi \mu_f^2 l_f \quad (14)$$

where

$$k_b = 1.3807 \times 10^{-23} \qquad (15)$$

k_b is the Boltzmann constant and l_f is the mean free path of water molecules that according to the suggestion of Chon *et al.* [15] is taken as 17nm. *df* is diameter of the base fluid molecules which is taken as 0.34nm for water. Mintsa *et al.* [16] have approved the accuracy of this model.

Viscosity of the nanofluid is approximated by the suggested correlation of Masoumi *et al.* [17]:

$$\frac{\mu_{nf}}{\mu_f} = 1 + \frac{\rho_p V_b d_p^2}{72 N \delta} \qquad (16)$$

Center to center distance of the nanoparticles and Brownian velocity of the nanoparticles are defined by:

$$\delta = \sqrt[3]{\pi/6\phi} \times d_p \qquad (17)$$

$$V_b = (1/d_p)\sqrt{18 k_b T / \pi \rho_p d_p} \quad (18)$$

N is a parameter for adapting the results with the experimental data, and is defined by:

$$N = (c_1\phi + c_2)d_p + (c_3\phi + c_4) \qquad (19)$$

$$c_1 = -1.133 \times 10^{-6}, \quad c_2 = -2.771 \times 10^{-6},$$
$$c_3 = 9.0 \times 10^{-8} \text{ and } c_4 = -3.93 \times 10^{-7}.$$

(20)

Density and specific heat of the nanofluid are calculated using the correlation provided by Pak and Cho [18], which are defined by:

$$\rho_{nf} = \phi\rho_p + (1-\phi)\rho_f \quad (21)$$

$$(c_p)_{nf} = \frac{(1-\phi) \times \rho_f \times (c_p)_f + \phi \times (\rho \times c_p)_p}{\rho_{nf}} \qquad (22)$$

Finally, the Nanofluid Prandtl number is:

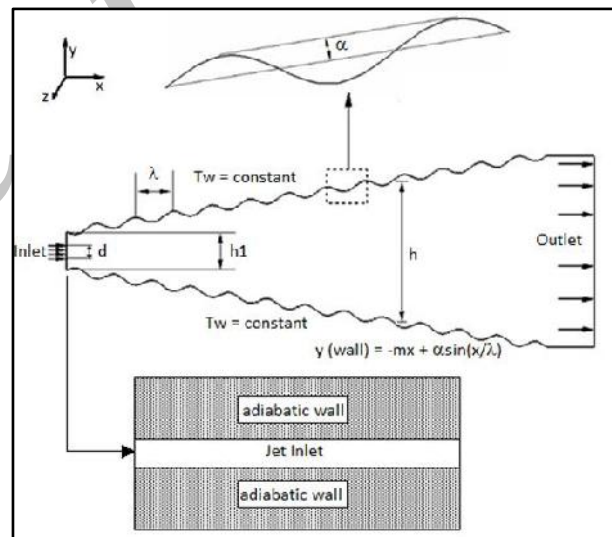$$\Pr_{nf} = \mu_{nf} \times c_{p_{nf}} / k_{nf} \qquad (23)$$

Fig. 1. Geometry of the problem

Numerical procedure and the code validation

A finite volume technique for collocated grids is implemented for discretizing the governing equations inside the computational domain. The SIMPLE algorithm is used to link pressure and velocity fields. For the stability of the solution, the diffusion term in the momentum equations is approximated by the central difference scheme. Moreover, a deferred correction scheme is adopted for the convective terms. An in-house code is

applied using the SIMPLE algorithm for laminar forced convection flow in a diverging sinusoidal channel. No quadrilateral element and non-uniform grid system are employed in the simulations. The grid is highly concentrated close to the jet in order to ensure the accuracy of the numerical simulation. In order to record the convergence history, the residual sum for each of the conserved variables is computed and stored. The convergence criterion requires that the maximum sum of the error for each of the conserved variables be smaller than 1×10^{-5}.

In order to validate the numerical methods used in this work, the numerical investigation performed by Wang and Chen [5] was used. The same problem was solved using the above mentioned methods, and the two results were compared. In Figure 2 the local Nusselt numbers along the duct are compared together. It is observed that a good agreement exists between these two results.
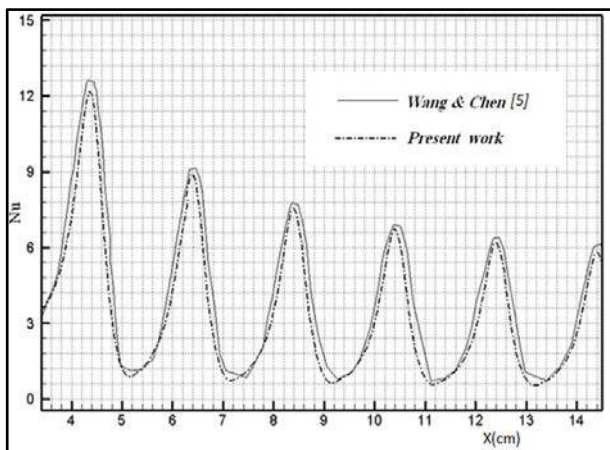
Fig. 2. Validation of the numerical methods using the work performed by Wang and Chen [5].

To perform a grid independence test, grid densities of 300×60, 400×80, 500×100 and 600×120 were used for computation. As shown in Figure3, for the largest grid (600×120) there is less than 1% difference in Nusselt numbers compared to the second largest grid (500×100). Therefore, the latter grid is selected for computation.
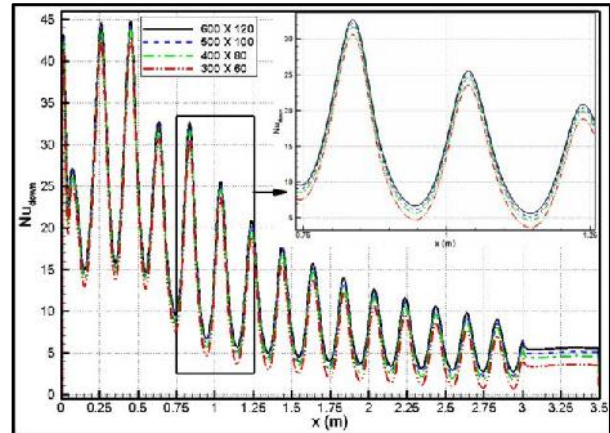

Fig. 3. Grid independence test.

RESULTS AND DISCUSSION

Computations were performed for the aspect ratios of 1, 2, 4 and 8, for the wavy-wall-profile amplitudes of 0.0, 0.01, 0.02, 0.03 and 0.04 meters, for the wavy-wall-profile wavelengths of 0.1, 0.2, 0.4, 0.8, 1.0 and 10 meters, for the Reynolds numbers of 25, 50, 75, 100, 125, 150, 175, 200, 225, 250, 275 and 300, for the Nanofluid volume fractions of 0%, 1%, 2%, 3%, 4% and 5% and for the nanoparticle diameters of 10, 25, 50, 75 and 100 nanometers.

In Figure 4 streamline patterns and temperature contours for Re=200, λ=0.2m, α=0.02m and $\phi = 0\%$ at different aspect ratios are depicted. In this work, aspect ratio is defined as the ratio of the inlet channel height to the jet height. The jet width is always equal to the channel width and only its height changes at different aspect ratios. It can be seen from the figure that at an aspect ratio of 1 at which the jet has the same size as the channel inlet, no separation is observed and the flow is uniform at each section of the channel. For aspect ratio of 2, back flow develops immediately after the sudden expansion, but it rapidly decays and the flow continues uniformly through the channel. In other words, transition from jet-to-duct flow occurs in a short distance. At a higher aspect ratio of AR=4, it is observed that the recirculation area is longer and wider, but after that the recirculation area decreases at AR=6. At very high aspect ratios such as AR=8, several eddies develop along the channel, and the flow is no

longer laminar and symmetrical. A variation of the local Nusselt number along the sinusoidal walls for different aspect ratios is shown in Figure 5. A large increase in Nusselt number can be seen in the vortex zone for aspect ratio of 4. Figure 6 shows the variation of averaged Nusselt number on the bottom wall with aspect ratio. It can be seen that heat transfer increases by about 20% when aspect ratio increases from 1 to 4. This enhancement is due to the development of recirculation zone in a large portion of the duct. Further increase of aspect ratio has an opposite effect on recirculation zone and hence on heat transfer.
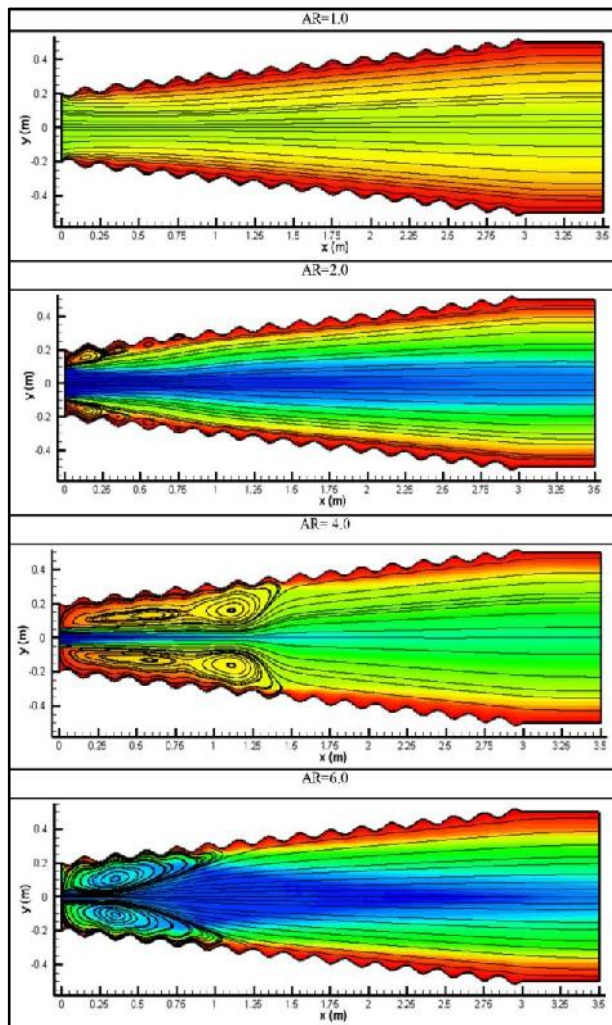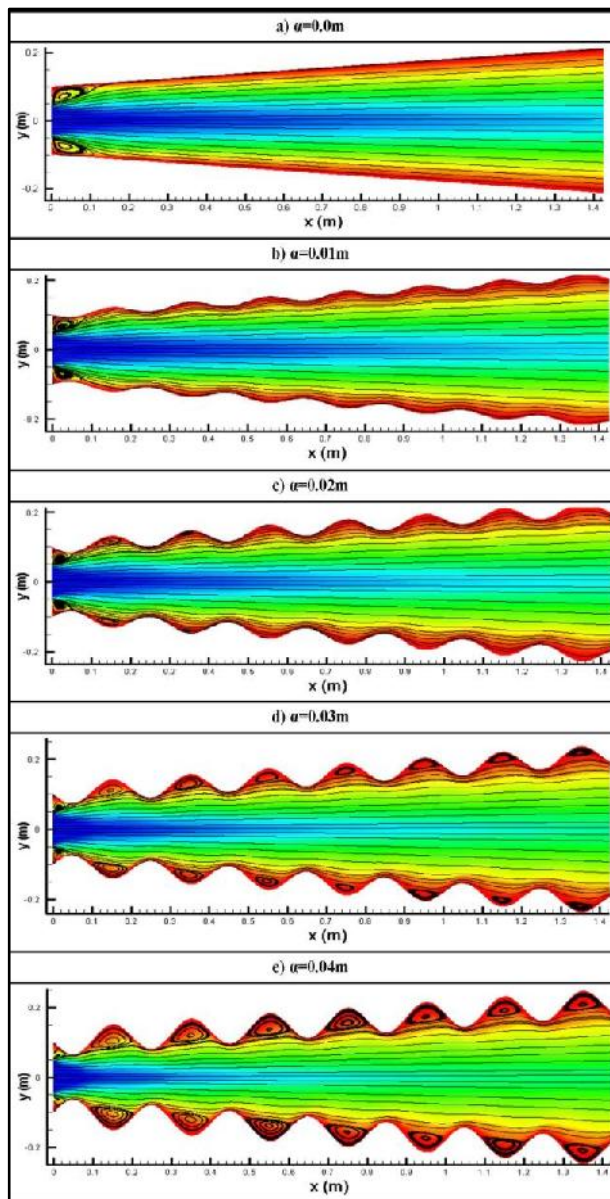

Fig. 4. Streamlines and temperature contours along the duct for different aspect ratios
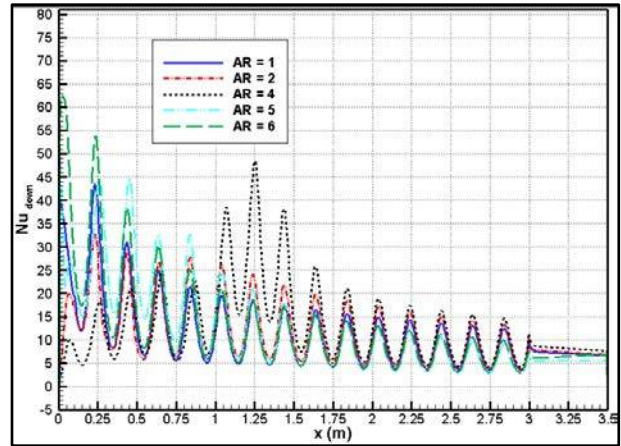
Fig. 5. Local Nusselt number along the duct for different aspect ratios.
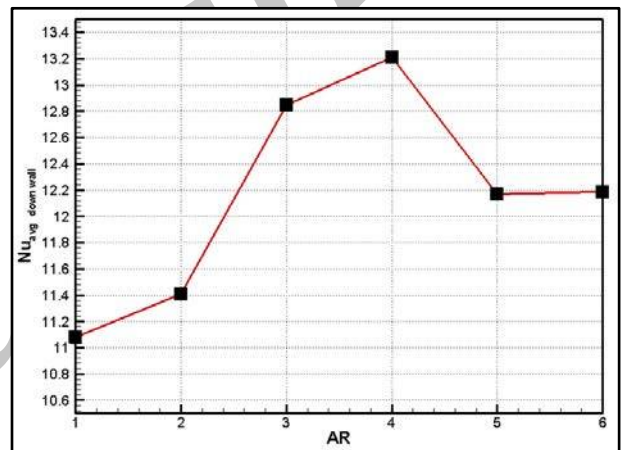
Fig. 6. Averaged Nusselt number on the sinusoidal walls versus aspect ratio.

In Figure7, the effects of the wall wave amplitude on the flow and temperature at Re=100, AR=2, λ=0.2m and $\phi = 0\%$ is investigated. It is observed that for zero and low amplitudes there is only a small recirculation zone right after the jet inlet due to sudden expansion, and there is no recirculation inside the wall waves. At higher amplitudes a recirculation zone forms in every wave of the sinusoidal wall. These recirculation zones have a large effect on increasing the local Nusselt number. This effect is shown in Figure 8 in which distribution of the Nusselt number along the upper wall for different amplitudes is drawn. It can be seen that for a flat wall (α=0) the curve smoothly declines along the channel length, and does not have any fluctuations. For the wavy walls the local

Nusselt number curves have a wavy shape while their trend is similar to the smooth curve related to the flat wall. In each wave of the Nusselt number curve, the peak occurs at the outward peak of the wall wave and the dip occurs at the inward peak of the wall wave. The amplitude of the waves of the local Nusselt number curves increases by increasing of the amplitude of the wall curves. The reason is that the size and strength of the recirculation flow inside the wall waves increase with increasing of amplitude, and hence heat transfer is enhanced.

Fig. 8. Local Nusselt number along the duct at different wall wave amplitudes.

Figure 9 shows the variation of the averaged Nusselt number on the lower and upper walls versus the wall-wave amplitude. As it was expected, heat transfer is enhanced by increasing of the amplitude. There is a 30% increase in heat transfer when flat walls are replaced by sinusoidal walls with amplitude of 0.04m.
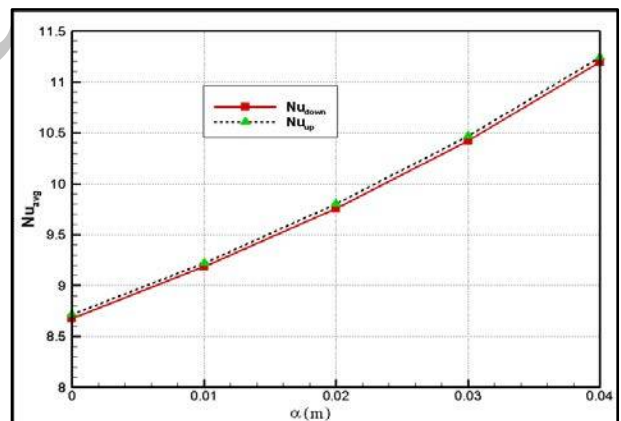

Fig. 9. Averaged Nusselt number on the sinusoidal walls versus wall wave amplitude.

In Figure 10, the effect of the wall wavelength on the flow and temperature fields at Re=100, AR=2, α=0.02m and $\phi = 0\%$ is investigated. At smaller wavelengths there are recirculation zones inside the wall waves, while for larger wavelengths the flow passes smoothly along the walls. The effect of the wall wavelength on the local Nusselt number along the wall is shown in

Fig. 7. Streamlines and temperature contours along the duct at different wall wave altitudes.

Figure 11. The local Nusselt number oscillates with the same wavelength as the wall, but its peak values decrease with the increase of the wavelength. The reason is that the recirculation zones inside the wall waves gradually vanish when the wavelength increases. The wall averaged Nusselt number is also decreased with the increase of the wall wavelength. As seen in Figure 12, the curve declines until the wavelength of 1m, and remains constant afterwards. Decrease of wavelength to 0.1m increases heat transfer by about 15%.
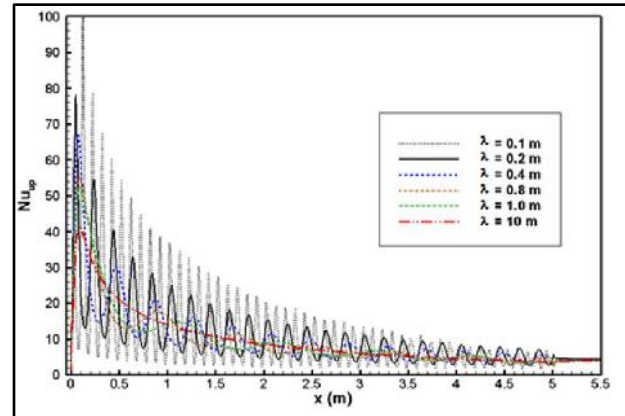

Fig. 11. Local Nusselt number along the duct at different wall wavelengths.

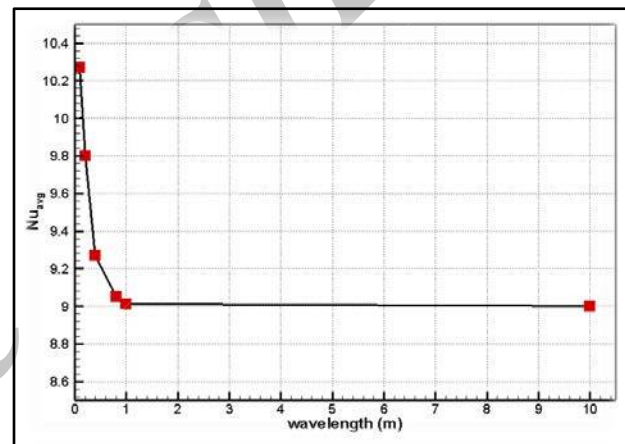**Fig. 12.** Averaged Nusselt number on sinusoidal walls versus wall wavelength.

Fig. 10. Streamlines and temperature contours along the duct for different wall wavelengths.

In Figure 13 the steady state streamline patterns and temperature contours at different Reynolds numbers are depicted for *AR*=2, λ=0.2, α=0.02m and $\phi = 0\%$. It is observed that for a low Reynolds number of *Re*=25 the jet development is symmetric and back flow velocities are only seen immediately after the sudden expansion. At a higher Reynolds number of *Re*=100, transition from jet-to-duct flow occurs over a longer distance. For the higher Reynolds numbers of 200 and 250, back flow is developed inside all the wall waves. As a result, the local Nusselt number should highly increase for large Reynolds numbers. This fact is shown in Figure 14. The averaged Nusselt number, as shown in Figure 15, increases by about 60% with increase of Reynolds number from 25 to 300.
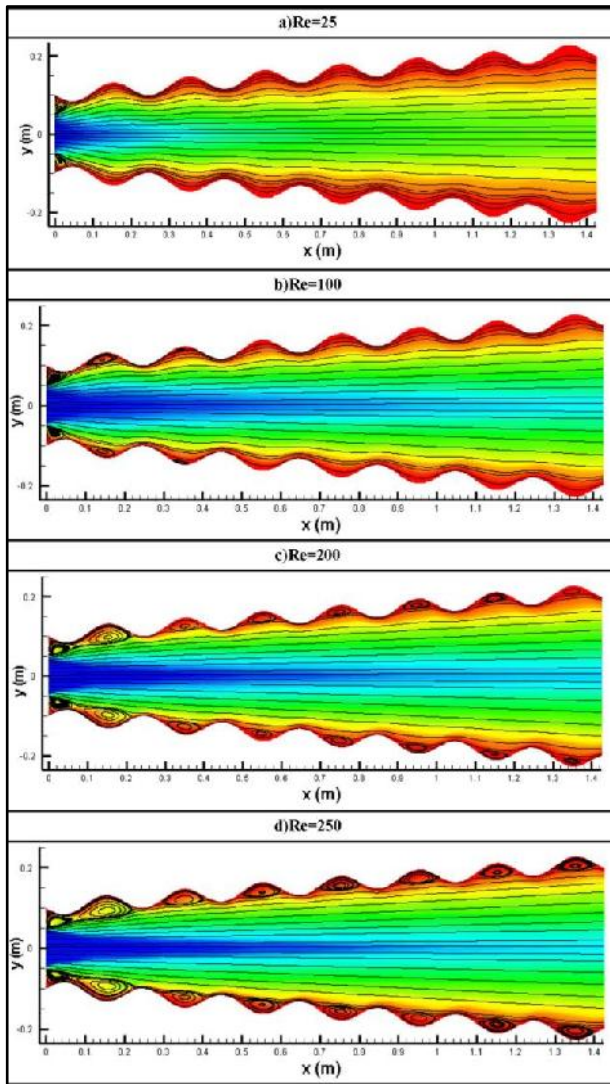
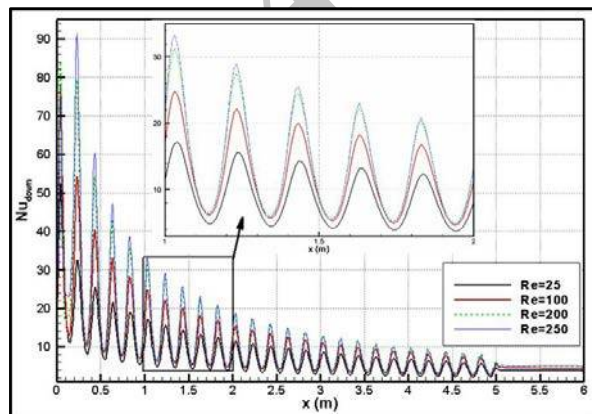**Fig. 13.** Streamlines and temperature contours along the duct for different Reynolds numbers.

Fig. 14. Local Nusselt number along the duct at different Reynolds numbers.
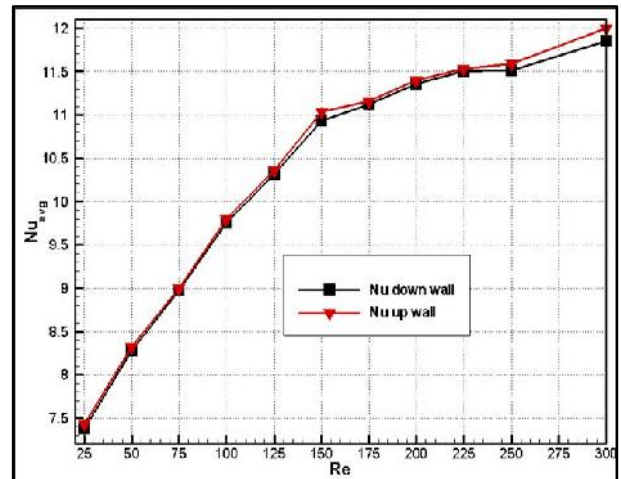

Fig. 15. Averaged Nusselt number on sinusoidal walls versus Reynolds number.

Figure16 shows the distribution of Nusselt number along the lower wall, using different nanoparticles volume fractions with *Re*=300, *AR*=2, λ=0.2m, α=0.02m and *dp*=36nm. This figure reveals an enhancement in heat transfer by the increase of the volume fraction of nanoparticles. This behavior can be inferred from equation (9), in which two terms of temperature gradient and thermal conductivity ratio are increased by increase of the volume fraction of nanoparticles. Temperature gradient increases due to increase of inertia forces. Inertia forces are increased by increase of ρ_{nf}, as depicted by equation (3), and ρ_{nf} increases by increase of $\emptyset$ according to equation (21). Besides, the nanoparticles increase the thermal conductivity ratio term which can be seen in equation (12). Figure 17 shows the particle volume concentration effects on the averaged Nusselt number on the lower and upper walls. It can be seen that the averaged Nusselt number for Re=100 increases by about 30% and for Re=300 increases by about 40% with increase of the nanoparticles volume concentration from 0 to 5%.

Figure 18 shows the effect of nanoparticles diameter on Nusselt number along the walls at *Re*=200, *AR*=2, λ=0.2m, α=0.02m and $\emptyset$=2%. Nusselt number gradually increases as the particles get smaller. Effect of particle size on the averaged Nusselt number is shown in Figure 19. It can be seen that by decrease of particles diameter from 100nm to 10nm, there is only 8% increase in

Nusselt number. This fact is confirmed by equation (12) which shows that thermal conductivity of nanofluid is inversely proportional to particle diameter to the power of 0.369.
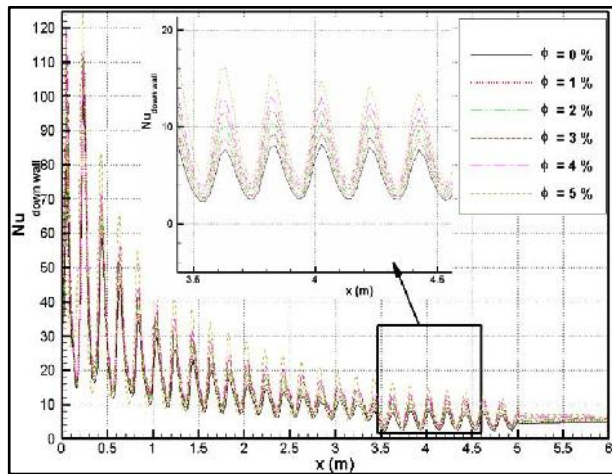

Fig. 16. Local Nusselt number along the duct for different nanoparticle concentrations
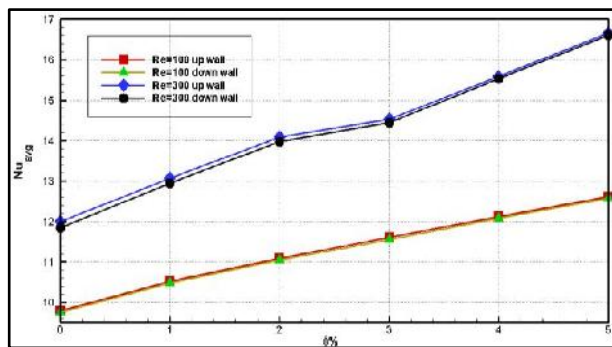

Fig. 17. Averaged Nusselt number on the sinusoidal walls versus nanoparticle concentration for two Reynolds numbers.
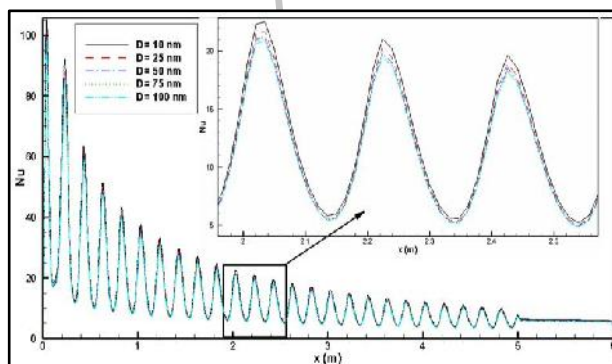

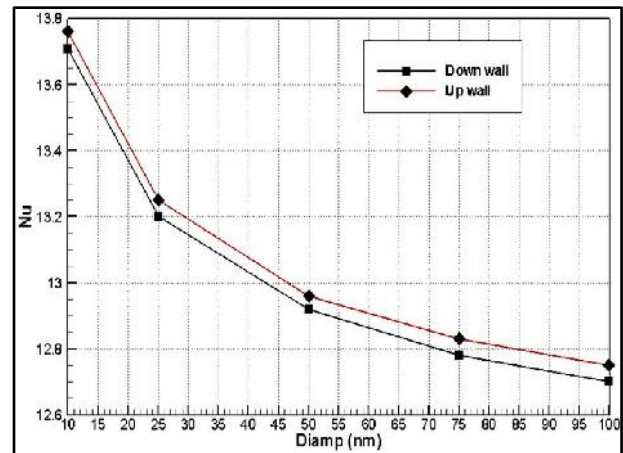**Fig. 18.** Local Nusselt number along the duct for different nanoparticle diameters.

Fig. 19. Averaged Nusselt number on the sinusoidal walls versus nanoparticle diameter.

CONCLUSIONS

Forced convection of laminar nanofluid flow in a diverging sinusoidal channel is numerically studied. The results showed that by increasing aspect ratio, wall wave amplitude and Reynolds number and by decreasing wall wavelength, the length and area of recirculation zones are increased. Furthermore, it was demonstrated that increase of the nanoparticle volume fraction and decrease of nanoparticles size, increase the fluid heat conductivity. Both recirculation growth and conductivity enhancement have an increasing impact on the local Nusselt number along the walls and a hence on the averaged Nusselt number of the duct. According to the results, Reynolds number has the highest effect, and the least effective parameter is the nanoparticle diameter.

In general, by increasing aspect ratio, wall wave amplitude, Reynolds number and nanoparticle volume fraction and by decreasing of nanoparticle diameter and wall wavelength, heat transfer between the channel walls and the fluid increases. Intensification of the turbulent eddies, suppression of the boundary layer, dispersion of the suspended particles, augmentation of the fluid thermal conductivity and heat capacity are suggested to be the possible reasons for heat transfer enhancement.

Nomenclature

C_p	specific heat (kJ/kg.K)
D	the jet height (m)
h	average height of the channel (m)
h_1	the channel inlet height (m)
K	thermal conductivity (W/m.K)
k_b	Boltzmann number (J/K)
L	the channel length (m)
$\dot{m}$	mass flow rate (kg/s)
$\hat{n}$	Unit vector normal to the surface
Nu	Nusselt number
P	pressure (Pa)
Pr	Prandtl number
Re	Reynolds number
T	temperature (K)
U	x component of the velocity (m/s)
V	y component of the velocity (m/s)
V_b	Brownian velocity of nanoparticles (m/s)

Greek symbols

α_f	thermal diffusivity (m²/s)
α	amplitude of the waves (m)
δ	center to center distance of nanoparticles (m)
ϕ	volume fraction of nanoparticles
λ	wavelength (m)
μ	viscosity (Pa.s)
υ	kinematic viscosity (m²/s)
ρ	density (kg/m³)

Subscripts

f	base fluid
in	channel inlet
Nf	nanofluid
P	Particle
W	Wall

ACKNOWLEDGMENTS

REFERENCES

[1] Choi S. U. S., (1995), Enhancing thermal conductivity of fluids with nanoparticles in developments and applications of non-Newtonian flows. *ASME FED 231/MD*. 66: 99–103.

[2] Keblinski P. P., Choi S. U. S., Eastman, J. A., (2002), Mechanisms of heat flow in suspensions of nano-sized particles (nanofluid). *Int. J. Heat and Mass Transfer*. 45: 855–863.

[3] Rahimi-Esbo M., Ranjbar A. A., Ramiar A. Arya A., Rahgoshay M., (2012), Numerical study of turbulent forced convection jet flow in a converging sinusoidal channel. *Int. J. of Therm. Sci.* 59: 176-185.

[4] Rahimi-Esbo M., Ranjbar A. A., Ramiar A., Rahgoshay M., Arya A., (2012), Numerical study of turbulent forced convection jet flow of nanofluid in a converging duct. *Int. J. Numer. Heat Transfer Part A: Appl.* 62: 33-41.

[5] Wang C. C., Chen C. K., (2002), Forced convection in a wavy-wall channel. *Int. J. Heat and Mass Transfer*. 45: 2587–2595.

[6] Ko T. H., Cheng C. S., (2007), Numerical investigation on developing laminar forced convection and entropy generation in a wavy channel, *Int. Communic. Heat and Mass Trans.* 34: 924–933.

[7] Oviedo-Tolentino F., Romero-Méndez R., Hernández-Guerrero A., Girón-Palomares B., (2008), Experimental study of fluid flow in the entrance of a sinusoidal channel, *Int. J. Heat and Fluid Flow*. 29: 1233–1239.

[8] Chang S. W., Lees A. W., Chou T. C., (2009), Heat transfer and pressure drop in furrowed channels with transverse and

skewed sinusoidal wavy walls, *Int. J. Heat and Mass Transfer.* 52: 4592–4603.

[9] Choi H. S., Suzuki K., (2005), Large eddy simulation of turbulent flow and heat transfer in a channel with one wavy wall. *Int. J. of Heat and Fluid Flow.* 26: 681–694.

[10] Heris S. Z., Etemad S. Gh., Esfahany M. N., (2007), Experimental investigation of convective heat transfer of Al$_2$O$_3$/water nanofluid in circular tube. *Int. Communic. Heat and Mass Transfer.* 28: 203–210.

[11] Hwang K. S., Jang S. P., Choi S. U. S., (2009), Flow and convective heat transfer characteristics of water-based Al$_2$O$_3$ nanofluids in fully developed laminar flow regime. *Int. J. Heat and Mass Transfer.* 52: 193-199.

[12] Al-Aswadi A. A., Mohammed H. A, Shuaib N. H., Campo A., (2010), Laminar forced convection flow over a backward facing step using nanofluids. *Int. Commun. in Heat and Mass Transfer.* 37: 950–957.

[13] Santra, A. K., Sen, S., Chakraborty N., (2009), Study of heat transfer due to laminar flow of copper–water nanofluid through two isothermally heated parallel plates. *Int. J. Therm. Sci.* 48: 391–400.

[14] Heidary H., Kermani M. J., (2010), Effect of nano-particles on forced convection in sinusoidal-wall channel, *Int. Commun. in Heat and Mass Transfer.* 37: 1520–1527.

[15] Chon C. H., Kihm K. D., Lee S. P., Choi S. U. S, (2005), Empirical correlation finding the role of temperature and particle size for nanofluid (Al2O3) thermal conductivity enhancement. *Appl. Phys. Lett.* 87: 153107–153110.

[16] Mintsa H. A., Roy G., Nguyen C. T., Doucet D., (2009), New temperature dependent thermal conductivity data for water-based nanofluids. *Int. J. of Therm. Sci.* 48: 363–371.

[17] Masoumi N., Sohrabi N., Behzadmehr A., (2009), A New model for calculating the effective viscosity of nanofluids. *J. Phys. D: Appl. Phys.* 42: 055501-055506.

[18] Pak B. C., Cho Y. I., (1998), Hydrodynamic and heat transfer study of dispersed fluids with submicron metallic oxide particles. *Experim. Heat Transfer.* 11: 151–170.

[19] Khoshvaght-Aliabadi M., (2014), Influence of different design parameters and Al2O3-water nanofluid flow on heat transfer and flow characteristics of sinusoidal-corrugated channels. *Energy Convers. and Manag.* 88: 96–105.

[20] Ahmed M. A., Yusoff M. Z., Ng K. C., Shuaib N. H., (2014), Effect of corrugation profile on the thermal–hydraulic performance of corrugated channels using CuO–water Nanofluid. *Case Studies in Therm. Engin.* 4: 65–75.

[21] Ahmed M. A., Shuaib N. H., Yusoff M. Z., (2014), Numerical investigations on the heat transfer enhancement in a wavy channel using Nanofluid. *Int. J. Heat and Mass Trans.* 23: 5891–5898.